APPENDIX – DATA REPOSITORY

To accompany Hannah et al., G23538, *Mo isotope variations in molybdenite: Vapor transport and Rayleigh fractionation of Mo*

Analytical Details

Molybdenum possesses seven stable isotopes of masses 92, 94, 95, 96, 97, 98, and 100, and thus offers multiple opportunities to measure natural mass fractionation. Potential isobaric interferences from ^{92,94,96}Zr and ^{96,98,100}Ru necessitate isolation of Mo from these elements to produce an extract suitable for mass spectrometry. Anbar et al. (2001) show that chemical purification of Mo by ion exchange can lead to isotopic fractionation unless Mo is recovered quantitatively. We overcome this potential problem by introducing a double spike enriched in ^{94}Mo and ^{100}Mo prior to ion exchange (Russell, 1971).

Each sample was dissolved in a 3:1 mixture of concentrated HCl and HNO_3, and purified by anion and cation exchange, to remove major cations, Ru, and Zr (details in Wieser and de Laeter, 2000). Extraction efficiency for the chemical separation was 93 ± 3%, and the full procedural blank for ion exchange chemistry was 7 ± 2 ng Mo. To correct for mass-dependent instrumental and chemical isotopic fractionation introduced during analysis, a double isotope spike of enriched ^{94}Mo and ^{100}Mo was added to each sample prior to ion exchange (spike composition in Table DR1). Although standard-sample bracketing, with or without addition of another element, may be used to monitor instrumental mass fractionation (Anbar et al., 2001; Pietruszka et al, 2006), the double-spike method eliminates the need for quantitative yields and also permits correction for mass fractionation incurred during chemical separation of Mo (e.g., Siebert et al., 2001; Wieser and de Laeter, 2003.

Mo isotope abundance ratios were measured using a ThermoElectron Neptune MC-ICPMS. For mass spectrometry, each purified Mo sample was diluted in 2M HNO_3 to a

concentration of ~200 ppb. Aspiration into a wet spray chamber at an uptake rate of 100 µl/min produced a $^{98}Mo^{+}$ signal of about 5V. About 200 ratios were collected in 20 blocks of 10 ratios each, followed by a three-minute washout with 2M HNO_3. The JMC Standard was analyzed repeatedly during the measurement regime to determine that the measured $^{98}Mo/^{95}Mo$ isotope ion current ratio of the standard drifted <0.008% over a 12-hour measurement session. Seven Faraday cup detectors were positioned to measure the seven stable isotopes of Mo, while two cups were aligned to monitor $^{90}Zr^{+}$ and $^{99}Ru^{+}$ ion beams that would signal potential isobaric interferences. No interferences from Zr or Ru, nor any polyatomic spectral interferences that overlap Mo isotope masses, were observed during the course of the measurements.

For data reduction, we follow the geometrical interpretation of double spike systematics outlined by Russell (1971), in which three sets of isotope ratios are combined to form a series of vectors, and linear algebra is used to calculate the magnitude of the isotopic fractionation relative to a laboratory standard. The laboratory standard solution used in this study, referred to throughout as the JMC Standard, was prepared from a 99.993% pure metal rod obtained from Johnson-Matthey Chemicals Ltd. (JMC 726, Laboratory No. S-8555; details in Wieser and de Laeter, 2000). The absolute isotopic composition for this standard has been measured and may be obtained from authors Wieser or de Laeter. Russell's procedure has been modified to give the uncertainty associated with each value of the isotopic fractionation using a Monte Carlo technique. Required program input data include the measured Mo isotope ratios of the JMC Standard, the double spike, a mixture of the JMC Standard with the double spike, and a mixture of each sample with the double spike. A reference value for isotopic fractionation is calculated from the spiked JMC Standard solution. The program output gives the fractionation in ‰/amu

for each molybdenite sample relative to the JMC Standard reference value. See details in Wieser and de Laeter (2003).

To test the reproducibility of the method, we prepared two different mixtures of our laboratory standard and the double spike (Mixtures A and B). Measured isotope ratios for the laboratory standard, the double spike, and the two mixtures are given in Table DR1. The fractionation of each sample relative to the JMC Standard based on the measured $^{98}Mo/^{95}Mo$ ratio was calculated twice, once for each standard-spike mixture (measured ratios given in Table DR2). The agreement of the two sets of results is excellent (Fig. DR1), so the means of the two calculated Mo isotope fractionation values (‰/amu) for each molybdenite sample are listed in Table 1 of the manuscript.

To assure that variations in the measured isotope ratios result from natural mass fractionation, $^{97}Mo/^{95}Mo$ and $^{98}Mo/^{95}Mo$ abundance ratios for each sample were calculated independently by the double spike algorithm and plotted as delta values relative to the JMC Standard (Fig. DR2). Least squares linear regression yields a line with a slope of 1.46 ± 0.03 and intercept of 0.01 ± 0.01, consistent with natural mass fractionation. There is no evidence that isobaric interferences significantly affected any of the measured isotope abundance ratios used in the calculations (94/95, 97/95, 98/95, and 100/95). Similarly, the double spike method effectively removes any mass-dependent fractionation resulting from sample preparation and analysis. Therefore, the results presented in the manuscript represent the natural variability of the Mo isotope composition of the samples themselves.

TABLE DR1. MEASURED Mo ISOTOPE RATIOS FOR SPIKES AND STANDARDS*

Sample	94/95	96/95	98/95	100/95
Lab Standard†	0.56795 (3)	1.07045 (3)	1.6187 (1)	0.67343 (9)
Double Spike	29.912 (5)	0.4532 (1)	0.5308 (1)	28.659 (4)
Mixture A	2.3262 (2)	1.03354 (9)	1.5538 (1)	2.3507 (2)
Mixture B	3.9979 (3)	0.99834 (9)	1.4917 (1)	3.9449 (4)

*One-sigma instrumental uncertainties are given in parentheses for the last digit indicated.
†Prepared from a Johnson Matthey Chemicals, Ltd., 99.993% pure Mo metal

TABLE DR2. MEASURED Mo ISOTOPE RATIOS FOR MIXTURES OF EACH MOLYBDENITE SAMPLE WITH DOUBLE SPIKE

Sample	94/95	96/95	98/95	100/95
CH02-LP1	1.77874 (28)	1.04474 (17)	1.57198 (32)	1.82249 (53)
CH02-LP13	1.58848 (22)	1.04904 (17)	1.58095 (25)	1.64521 (26)
SW02-SK1	1.52697 (12)	1.05011 (9)	1.58241 (20)	1.58573 (35)
SW02-SK2	1.66053 (10)	1.04763 (7)	1.57891 (25)	1.71586 (44)
SW02-SK3	1.32904 (7)	1.05457 (6)	1.59108 (11)	1.39948 (11)
NW01-KS1	1.75024 (11)	1.04561 (7)	1.57501 (11)	1.80030 (11)
NW01-KS2	1.66009 (11)	1.04764 (8)	1.57901 (11)	1.71510 (12)
NW01-KS3	2.69592 (22)	1.02562 (10)	1.53946 (13)	2.70070 (25)
NW97-LG3	1.37292 (9)	1.05362 (6)	1.58934 (14)	1.44128 (19)
NW00-LG7	1.16752 (6)	1.05804 (6)	1.59739 (9)	1.24575 (9)
GE99-HE1	1.45977 (9)	1.05158 (8)	1.58482 (13)	1.52247 (15)
Seinargiu 1	1.35331 (12)	1.05418 (9)	1.59066 (14)	1.42315 (15)
Seinargiu 2	1.13008 (7)	1.05896 (7)	1.59936 (10)	1.21056 (10)
Flumini Binu	1.09360 (7)	1.05969 (7)	1.60058 (10)	1.17574 (8)
DDH 319	1.60405 (12)	1.04885 (10)	1.58119 (15)	1.66187 (18)
OTRCD150	2.28075 (21)	1.03435 (11)	1.55484 (16)	2.30534 (27)
ORBD-49 (1)	1.03936 (9)	1.06040 (7)	1.60062 (11)	1.12236 (12)
ORBD-49 (2)	1.43868 (11)	1.05228 (9)	1.58692 (21)	1.50346 (27)
Edna May (2)	1.38660 (9)	1.05358 (6)	1.58853 (10)	1.45187 (12)
Harbour Lights	1.31915 (9)	1.05462 (7)	1.59069 (11)	1.38892 (11)

*Standard deviation for last digits indicated in parentheses.

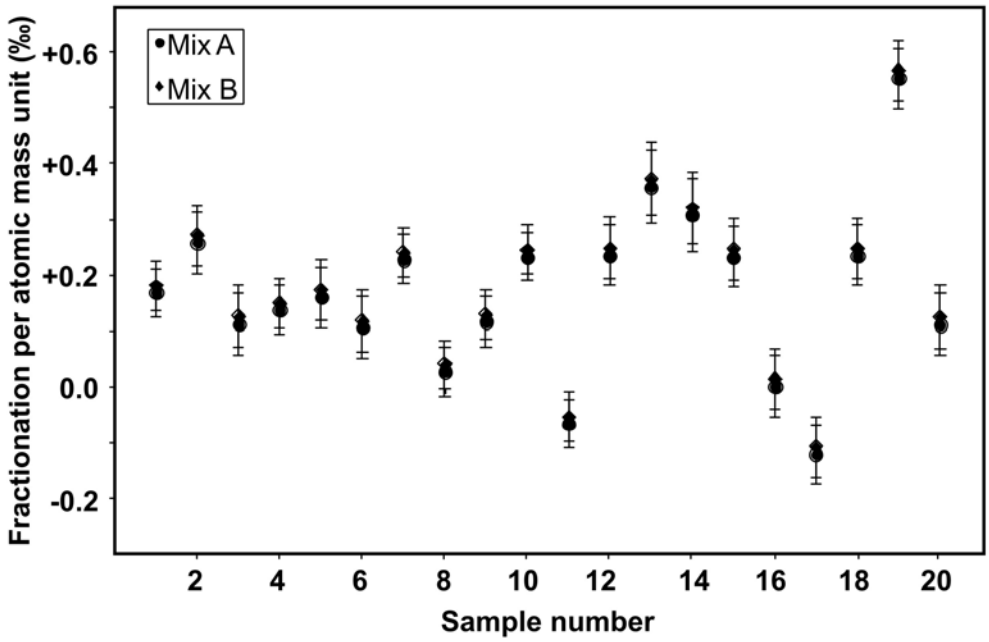

Figure DR1: Mo isotope fractionation (in ‰/amu) for twenty molybdenites. Two points are plotted for each sample, representing the calculated isotopic fractionation values based on Mixtures A and B of the in-house JMC standard plus the double spike. Error bars are one-sigma.

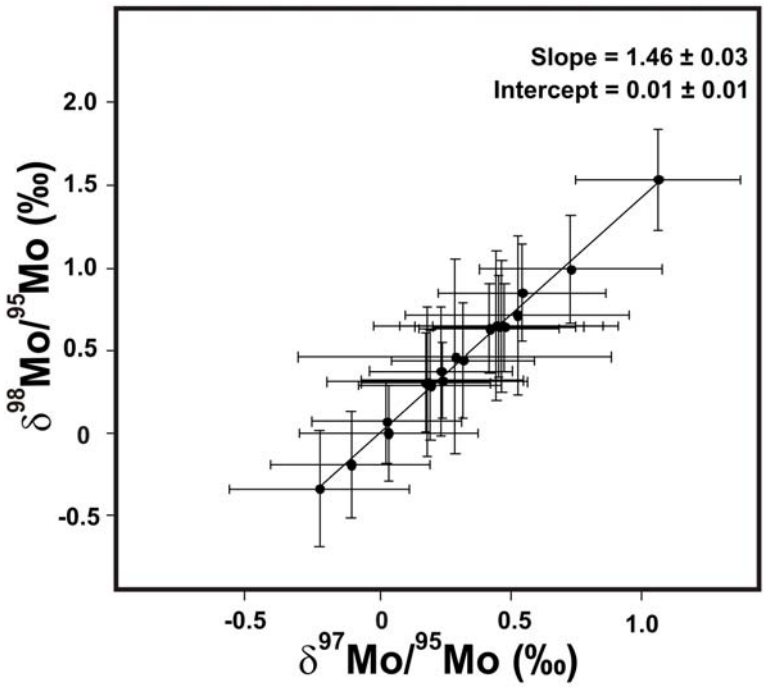

Figure DR2. Comparison of $\delta^{98/95}$Mo and $\delta^{97/95}$Mo, calculated independently from measured ratios for each sample. Least squares linear regression yields the slope and intercept expected for mass-dependent fractionation. The excellent fit demonstrates the high precision, lack of isobaric interferences, and appropriate corrections for chemically or analytically induced mass fractionation. Error bars are 1σ.

Geologic Description of Molybdenite Samples and Other Information

Los Pelambres, Chile

Los Pelambres is one of the world's major porphyry Cu deposits located on the Chile-Argentina border. Sample **CH02-LP1** (MDID-31) is a planar B-style vein from the Cachimba Norte sector of the open pit. Coarse crystalline molybdenite occurs on the margins of quartz veins, with trace quantities of pyrite + chalcopyrite. No alteration halo is present around vein, but host intrusion displays potassic alteration. These quartz veinlets cut earlier biotite-bearing veinlets, and quartz infilling may locally show open space textures. Sample **CH02-LP13** (MDID-23) is an early 0.2 cm EB-style vein (early biotite) from the 3065 N bench of the open pit. Quartz + molybdenite + coarse-grained biotite + minor chalcopyrite constitute the vein composition. No alteration envelope is present about the vein. This EB vein is cut by a B veinlet. Sample collected by H. Stein with R. Sillitoe, and P. Perelló in February 2002.

Särkivaara, N Sweden

Three samples were obtained the Särkivaara Cu-Au deposit associated with metadiabase, mafic tuffite, and marble, Norrbotten, northern Sweden. The massive to disseminated pyrite + chalcopyrite + pyrrhotite + molybdenite ore occurs in a high-temperature scapolite ± biotite skarn that is associated with the metadiabase. Sample **SW02-SK1** (MDID-141) is fine-grained molybdenite in calc-silicate skarn with chalcopyrite + epidote + magnetite, sample **SW02-SK2** (MDID-152) consists of a molybdenite patch in coarse-grained pyroxene skarn with chalcopyrite rimming euhedral pyroxene, and sample **SW02-SK3** (MDID-153) contains a molybdenite patch in massive scapolite rock with 10% epidote and minor chalcopyrite. Samples were collected

from the Särkivaara mine dump with colleagues Pär Weihed and Olof Martinsson from Luleå University (Sweden) in 2002.

Konstali, S Norway

The Konstali mine is situated in the Sira district of S Norway near the orthopyroxene-in isograd associated with the Rogaland anorthosite intrusion (Bingen et al., 2006). The host is banded augen gneiss. Sample **NW01-KS1** (MDID-448A) is foliation-parallel molybdenite from a medium-grained amphibolite. KS1 was taken from the nose of a 10 cm amplitude fold in the amphibolite. Sample **NW01-KS2** (MDID-442A) and **NW01-KS3** (MDID-449A) are from a prominent 20 cm, foliation parallel, zoned quartzofeldspathic vein. The vein is very coarse-grained with a pegmatite quality. KS2 was taken from the central quartz-rich part of the vein, and KS3 was collected from the marginal feldspar-rich part. For both K2 and K3, molybdenite crystals form aggregates that are poorly-oriented and <1 cm in size. All samples were collected from blocks of mine material located just at the adit entry point. Samples were collected in 2001 by H. Stein, J. Hannah, and B. Bingen in a driving Norwegian rain.

Langvatn-Kobberknuten, S Norway

Samples were taken from a pair of Cu-Mo prospects hosted in a epidote-amphibolite facies metagabbro-metabasalt of the Sæsvatn supracrustal sequence, in S Norway (Stein and Bingen, 2002). Sample **NW97-LG3** (CT-233) is from a zone of ductile deformation in a sill of metagabbro (coarse-grained amphibolite). The molybdenite at this location is kinked and recrystallized within single blades and laths, and gangue minerals quartz + calcite have marked undulatory extinction in this section. Sample **NW00-LG7** (CT-304) about 2 km away is from a

brittle vein-fracture that cross-cuts fine-grained metabasalts residing higher in the stratigraphic section. The basalt hosts small clots to irregular veinlets of calcite + quartz + epidote + amphibole ± pyrite ± chalcopyrite, cm-scale bornite ± chalcopyrite patches, and 2-5 mm pristine molybdenite blades within and cutting the basalt foliation. LG7 consists of delicate molybdenite blades and rosettes that clearly cross-cut the foliation and post-date all deformation. LG3 was obtained from the collection of Frank Vokes; LG7 was collected by H. Stein and B. Bingen in September 2000.

Henneberg, Germany

The massive, undeformed, medium-grained Henneberg granite is exposed in a quarry in southernmost Thüringen, Germany. The pink biotite granite to gray muscovite granite resides in the Variscan orogenic belt along the northwest margin of the Bohemian massif. Minor molybdenite mineralization has been observed at a few locations in the quarry. The molybdenite is highly localized and is vein-hosted, vein/vug-hosted, and occurs as radiating disseminations. Sample **GE99-HE1** (CT-209A) consists of 0.3 to 0.5 cm molybdenite rosettes from a 1 cm UST band in the gray granite. The Re-Os age is in excellent agreement with a 299 ± 6 Ma U-Pb age for the Henneberg granite (Loth et al., 1999). This sample is part of a larger sampling and study conducted by H. Stein and R. Höll, and was provided by K. Bartzsch.

Sardinia, Italy

The southwest part of Sardinia hosts small W-Mo-(Sn)-(Ni-Co)-(Fe-Cu-Zn-Pb) deposits associated with felsic magmatic rocks of the Variscan Sardinia-Corsica batholith. The batholith is hosted in Early Paleozoic shales. Leucogranite porphyritic rocks are cut by aplite dikes ±

large quartz veins. Shear zones are locally associated with leucogranite localities. Argillic alteration with lesser sericitic alteration is widespread in mineralized regions. The molybdenite most commonly occurs in quartz veins, but is also present as disseminations in porphyritic rocks. Pyrite and chalcopyrite, plus less common wolframite, may accompany molybdenite. The Su Seinargiu and Flumini Binu (Teulada) W-Mo deposits are contained in the Sulcis mining district (Boni et al., 2003). Two samples from the **Su Seinargiu** (1 and 2) and a sample from the **Flumini Binu** deposit were analyzed in this study. Because the Su Seinargiu 1 and Flumini Binu samples contained red Fe oxide intergrown with the molybdenite, Re loss has disturbed the Re-Os ages. The Re-Os age for fresh molybdenite from Su Seinargiu 2 (MDID-85) is in excellent agreement with U-Pb ages for magmatic rocks of the Corsica-(Sardinia) batholith (Cocherie et al., 2005). The mine dump samples for this study were obtained from M. Boni.

Oyu Tolgoi, Mongolia

The size and scale of the Cu-Au porphyry system at Oyu Tolgoi was not recognized until the last decade. There are four related deposits constituting Oyu Tolgoi, the Central Oyu, South Oyu, Southwest Oyu, and Au-rich Hugo Dummett (North and South Hugo) deposits (Kirwin et al., 2005). Both molybdenite samples, from the **Southwest Oyu** (CT-543A) and the **Hugo North** (MDID-164), are associated with immensely altered (advanced argillic-sericitic) fine-grained porphyritic quartz monzodiorite host rock. At the Southwest Oyu, the deposit is centered on a small quartz monzodiorite stock intruded into massive biotite and magnetite altered porphyritic augite basalt. The basalt hosts 80% of the Cu and Au mineralization. The molybdenite sample from Hugo North is hosted in a highly chloritized and brecciated greenstone, probably basalt. The Hugo North mineralization is also associated with a quartz monzodiorite exhibiting a high

degree of silicification, argillization, and sericitization. A high sulfidation zone overlies the bulk of the deposit. The molybdenite samples used in this study were provided by D. Kirwin as part of a dating study to temporarily link deposits as the size and scope of the Oyu Tolgoi system was being delineated by Ivanhoe Mines.

Ora Banda (Enterprise), Yilgarn, Australia

The Ora Banda Au ore field is associated with a folded ultramafic sequence underlain by a buried granite intrusion. A small aphophyse of the granite intrusion outcrops about 200 meters north of the Enterprise deposit. Specifically, the Enterprise deposit is situated within the top portion of the Enterprise dolerite sill, where it is intersected by a vertical E-W striking fault. The Au is associated with disseminated pyrite within a chlorite-sericite-ankerite alteration system. The molybdenite analyzed (CT-479A, CT-491A) is from drill core sample **ORBD 49**, 235.2-235.5 meters. The molybdenite is contained in an ultramafic clast within a late ankerite vein. Both Au and Mo have the same gross spatial distribution at Enterprise. Two different separates were prepared of like occurrences of molybdenite from this clast for Mo isotope analyses and Re-Os dating. The sample was obtained from S. Halley who also provided detailed documentation.

Edna May, Yilgarn, Australia

The Edna May Au deposits, also known as the Westonia Au deposits, are located in the Southern Cross region of the Yilgarn craton in southwest Australia. The molybdenite is hosted in quartz reef structures associated with the Edna May tonalitic gneiss sandwiched between a hanging wall and footwall of ultramafic rocks (Drummond and Beilby, 1990). The Edna May gneiss is

believed to be part of the regional greenstone sequence and was emplaced as a tonalite along a shear controlled fracture. The gold occurs with tungsten and sulfide mineralization and is believed to have a primary magmatic origin. Subsequently, as the tonalite underwent progressive shear deformation, gold was remobilized into major vein and reef structures (Drummond and Beilby, 1990). The molybdenite used in this study, **Edna May 2** (CT-163A), is from the Western Australian Museum (300 mg piece off S1743A), and was prepared and sent by A. Bevan. The sample is from the Central Reef in the Edna May gneiss. The analyzed sample was arranged by A. Müller courtesy of G. Hall, Placer Dome.

Harbour Lights, Yilgarn, Australia

The Harbour Lights Au deposit is located in the Archean Yilgarn block, southwestern Australia. It is located in the Eastern Goldfields province and is the northernmost of three significant Au deposits among numerous prospects forming the Leonora district. Although the Harbour Lights deposit is surficially hosted in potassically altered talc-chlorite-carbonate schist, the mineralization is situated along the east margin of the foliated granite-monzogranite constituting the Raeside batholith. The **Harbor Lights** molybdenite sample is from a piece of drill core residing in the collection of University of Western Australia (DDH HL347, 155.87-155.95 m, 103087). The analyzed molybdenite (CT-82A) is hosted in porphyry, and occurs as small (2-5 mm) disseminated clots in a quartz vein cutting the porphyry. Sample is from Skwarnecki's thesis collection. The sample was acquired in the mid-1990s from P. Duuring.

References in Supplementary Documentation

Anbar, A.D., Knab, K.A., and Barling, J., 2001, Precise determination of mass-dependent variations in the isotopic composition of molybdenum using MC-ICPMS: Analytical Chemistry, v.73, p. 1425-1431.

Bingen, B., Stein, H.J., Bogaerts, M., Bolle, O., and Mansfeld, J., 2006, Molybdenite Re-Os dating constrains gravitational collapse of the Sveconorwegian orogen, SW Scandinavia: Lithos, v. 87, p. 328-346.

Boni, M., Stein, H.J., Zimmerman, A., and Villa, I.M., 2003, Re-Os age for molybdenite from SW Sardinia (Italy): a comparison with $^{40}Ar/^{39}Ar$ dating of Variscan granitoids, *in* Eliopoulos, D.G. et al., eds., Mineral Exploration and Sustainable Development: Rotterdam, Millpress, p. 247-250.

Cocherie, A., Rossi, P., Fanning, C.M., and Guerrot, C., 2005, Comparative use of TIMS and SHRIMP for U-Pb zircon dating of A-type granites and mafic tholeiitic layered complexes and dykes from the Corsican batholith (France): Lithos, v. 82, p. 185-219.

Drummond, A.J. and Beilby, G.R., 1990, Westonia gold deposits, *in* Hughes, F.E. (editor), Geology of the Mineral Deposits of Australia and Papua New Guinea: The Australasian Institute of Mining and Metallurgy, Melbourne, p. 289-295.

Kirwin, D., Forster, C.N., Kavalieris, I., Crane, D., Orssich, C., Panther, C., Garamjav, D., Mankhbat, T.O., and Niislelkhuu, G., 2005, The Oyu Tolgoi copper-gold porphyry deposits, South Gobi, Mongolia, in Seltmann, R., Gerel, O., and Kirwin, D. (eds.), Geodynamics and Metallogeny of Mongolia, with special emphasis on copper and gold deposits: International Association on the Genesis of Ore Deposits (IAGOD), Guidebook Series, v. 11, London.

Loth G., Höll, R., Ritter-Höll, A., Bartzsch, K., and Kennedy, A., 1999, U-Pb SHRIMP-Alter von Zirkonen aus einem Biotit-Granit der Henneberg-Intrusion (Thüringen): Beitr. Geol. Thüringen, N.F.6, 3 Abb, p. 209-215.

Pietruszka, A.J., Walker, R.J., and Candela, P.A., 2006, Determination of mass-dependent molybdenum isotopic variations by MC-ICP-MS: An evaluation of matrix effects: Chemical Geology, v. 225, p. 121-136.

Russell, R.D., 1971 The systematics of double spiking: Journal of Geophysical Research, v. 76, p. 4949-4955.

Siebert, C., Nägler, T.F., and Kramers, J.D., 2001, Determination of molybdenum isotope fractionation by double-spike multicollector inductively coupled plasma mass spectrometry: Geochemistry Geophysics Geosystems 2, 2000GC000124.

Stein, H.J. and Bingen, B., 2002, 1.05-1.01 Ga Sveconorwegian metamorphism and deformation of the supracrustal sequence at Sæsvatn, south Norway: Re-Os dating of Cu-Mo mineral occurrences, in Blundell, D., Neubauer F., & von Quadt, A. (eds.), The Timing and Location of Major Ore Deposits in an Evolving Orogen: Geological Society, London, Special Publications, 204, p. 319-335.

Wieser, M.E., and de Laeter, J.R., 2000, Thermal ionization mass spectrometry of molybdenum isotopes: International Journal of Mass Spectrometry, v. 197, p. 253-261.

Wieser, M.E., and de Laeter, J.R., 2003, A preliminary study of isotope fractionation in molybdenites: International Journal of Mass Spectrometry, v. 225, p. 177-183.